

REPORT DOCUMENTATION PAGE

1a. REPORT SECURITY CLASSIFICATION <b>Unclassified</b>		1b. RESTRICTIVE MARKINGS	
2a. SECURITY CLASSIFICATION AUTHORITY  JLE		3. DISTRIBUTION / AVAILABILITY OF REPORT Approved for public release; distribution unlimited.	
<b>AD-A199 992</b>		5. MONITORING ORGANIZATION REPORT NUMBER(S) <b>AFOSR-TR- 88-0991</b>	
6a. NAME OF PERFORMING ORGANIZATION Stanford University		7a. NAME OF MONITORING ORGANIZATION Air Force Office of Scientific Research	
6b. OFFICE SYMBOL (If applicable)		7b. ADDRESS (City, State, and ZIP Code) <b>Bldg 410</b> Bolling Air Force Base, DC 20332-6448	
6c. ADDRESS (City, State, and ZIP Code) Applied Physics Department Stanford University Stanford, California 94305		8a. NAME OF FUNDING / SPONSORING ORGANIZATION AFOSR	
8b. OFFICE SYMBOL (If applicable) NP		9. PROCUREMENT INSTRUMENT IDENTIFICATION NUMBER AFOSR-86-0275	
8c. ADDRESS (City, State, and ZIP Code) <b>Bldg 410</b> Bolling Air Force Base, DC 20332-6448		10. SOURCE OF FUNDING NUMBERS	
		PROGRAM ELEMENT NO. 61102F	PROJECT NO. 2917
		TASK NO. A6	WORK UNIT ACCESSION NO.
11. TITLE (Include Security Classification) Tunable Solid State Lasers and Synthetic Nonlinear Materials			
12. PERSONAL AUTHOR(S) Robert L. Byer			
13a. TYPE OF REPORT Final Technical	13b. TIME COVERED FROM 8/1/86 TO 7/31/87	14. DATE OF REPORT (Year, Month, Day) September, 1987	15. PAGE COUNT 45
16. SUPPLEMENTARY NOTATION			
17. COSATI CODES		18. SUBJECT TERMS (Continue on reverse if necessary and identify by block number)	
FIELD	GROUP	Spectrometer System, Mass Spectrometers, optical equipment, Automated Microscopy System, Superconducting (magn)	
19. ABSTRACT (Continue on reverse if necessary and identify by block number) This document is the final report for Instrumentation Grant #AFOSR-86-0275, an award of \$342,306 for the time period 8/1/86 to 7/31/87. The report contains five (5) sections: I) a list of equipment proposed and purchased under the grant, II) a discussion of exceptions to the original equipment list, III) a summary of the research projects on which the equipment has been used, IV) a synopsis of the ongoing research activities of the Byer group, and V) a summary.			
20. DISTRIBUTION / AVAILABILITY OF ABSTRACT <input checked="" type="checkbox"/> UNCLASSIFIED/UNLIMITED <input checked="" type="checkbox"/> SAME AS RPT. <input type="checkbox"/> DTIC USERS		21. ABSTRACT SECURITY CLASSIFICATION Unclassified	
22a. NAME OF RESPONSIBLE INDIVIDUAL Howard Schlossberg		22b. TELEPHONE (Include Area Code) 202-767-4906	22c. OFFICE SYMBOL NP

**DTIC ELECTED**  
**S** OCT 06 1988 **D**  
 H

**AFOSR-TR- 88-0991**

**Edward L. Ginzton Laboratory  
Stanford University  
Stanford, CA 94305**

**Final Report to the  
Department of the Air Force**

**TUNABLE SOLID STATE LASERS  
AND SYNTHETIC NONLINEAR MATERIALS  
(AFOSR-86-0275)**

**Robert L. Byer  
Principal Investigator  
Applied Physics Department  
Stanford University  
Stanford, CA 94305  
(415) 723-0226**

**STANFORD UNIVERSITY**

**4 2 6 7**

**GINZTON LABORATORY  
G. L.**

**September 1987**

**08 10 5 211**

**ABSTRACT**

This document is the final report for Instrumentation Grant No. AFOSR-86-0275, an award of \$342,306 for the time period 8/1/86 to 7/31/87. The report contains five sections: I) a list of equipment proposed and purchased under the grant, II) a discussion of exceptions to the original equipment list, III) a summary of the research projects on which the equipment has been used, IV) a synopsis of the ongoing research activities of the Byer group, and V) a summary.

**I. LIST OF EQUIPMENT PURCHASED UNDER THE GRANT**

Below are A) the originally proposed equipment list, and B) the the list of the equipment actually purchased under the grant. The latter list gives the name of the purchased item, the manufacturer, and the cost. Discussion of special circumstances and exceptions to the originally proposed equipment list are deferred to section II.

**A) Proposed Equipment List**

(from June 1986 revision of "Tunable Solid State Lasers and Synthetic Nonlinear Materials" )

<u>Item</u>	<u>Estimated Cost</u>
<b>FTIR spectrometer and associated equipment</b>	
IBM IR/32 FTIR Spectrometer System with Automated Microscopy System	80,500.
<b>Specific research instruments</b>	
Gaertner Research Spectrometer	11,500.
Pyroelectric Vidicon Camera & 50 mm Lens	12,495.
HP 8568B RF Spectrum Analyzer	34,600.
SpectraLase 50 Q-Switched Grating Tuned Carbon Dioxide Laser	29,800.
Spectra-Physics Quanta-Ray DCR-2A(10) Nd:YAG Laser	48,000.



Session For	
NS GR&I	<input checked="" type="checkbox"/>
NS TAB	<input type="checkbox"/>
Unannounced	<input type="checkbox"/>
Classification	
Distribution/	
Availability Codes	
Dist	Avail and/or Special
A-1	

**Equipment for the Optics Shop**

6CR 36 inch Polishing Machine & Laps	8,665. 1,335.
7Y Ultraprecision Curve Generator	31,945.
Digital Spindle Height	2,180.
Digital Head Angle	2,180.
Variable Speed Spindle	1,120.
LOH Spherometer Set	3,700.
6DE Grinding & Polishing Machine with One Spindle	3,840.
Micromech Semi-automatic Precision Wafering Machine	33,988.
Levin Micro Drilling Unit	4,760.
Hardinge Super Precision Lathe	11,698.
Carl Zeiss Invertoscope M, with Various Objectives for DIC Interference	20,000.
	<hr/>
Total:	342,306.

**B) Equipment Purchased****FTIR spectrometer and associated equipment**

FTS 40 FT-IR System #099-0749 with a) Broadband MCT Detector #099-0743 b) External Beam Option #099-0744 c) IR-plan-1 Microscope Side-port version with narrow band MCT detector manufacturer: Digilab Division, BioRad	70,741.
K770T Cryogenic Refrigeration System for Optical Transmission, with temperature controller manufacturer: MMR Technologies	3,505.
2 Wiregrid Polarizers (ZnSe) Ar-coated for 5-11 microns & 2 ZnSe Ar-coated windows (1 inch dia.) manufacturer: PTR Optics	4,680. 800.
Photovoltaic InSb detector for wavelength region 4.5-5.5 microns manufacturer: Infrared Associates, Inc.	1,706.

Two Stage Vacuum Pump #8804B 413.  
 manufacturer: Sargent-Welch Scientific Co.

#### Specific research instruments

KNS series table top, 4'x12'x12" Model KNS412-12 5,467.  
 with non-isolating support system (four 28" legs)  
 manufacturer: Newport Corporation

8600-01 Model 86 Thermal Imaging System with 13,584.  
 8650-01 TH-9873 ZnSe Pyroelectric Vidicon &  
 8601-25 25 mm lens  
 manufacturer: ISI Group, Inc.

71100A Spectrum Analyzer with Rack Mount 32,880.  
 manufacturer: Hewlett Packard

Spectralase 50 Q-switched Grating Tuned 29,890.  
 Carbon Dioxide Laser  
 manufacturer: Advanced Kinetics, Inc.

Quanta-Ray DCR-3D(30) Nd:YAG pulsed laser system 59,694.  
 manufacturer: Spectra-Physics

#### Equipment for Optics Shop

Emco coordinate drilling and milling machine 3,989.  
 Model No. 760.1 RB  
 manufacturer: Emco

Slicing & Dicing Machine with accessories 32,975.  
 Spherometer set 3,665.  
 manufacturer: LOH Optical Machinery

6CR 36 inch Polishing Machine & Laps 9,595.  
 manufacturer: R. Howard Strasbaugh, Inc.

7Y Ultraprecision Curve Generator & accessories 37,315.  
 manufacturer: R. Howard Strasbaugh, Inc.

6DE Grinding & Polishing Machine with one spindle 6,046.  
 & accessories for above  
 manufacturer: R. Howard Strasbaugh, Inc.

Microscope accessories 9,014.  
 manufacturer: Carson Optical Instruments, Inc.

Levin Micro-Drilling Attachment with Idler Attachment & "WW" Collet set manufacturer: Louis Levin and Son, Inc.	4,667.
Hardinge super precision shop lathe with grinder and universal chuck manufacturer: Hardinge Bros. Inc.	11,680.
	-----
<b>Total :</b>	<b>342,306.</b>

## II. SPECIAL CIRCUMSTANCES AND EXCEPTIONS TO ORIGINAL EQUIPMENT LIST

The equipment list given in the proposal "Tunable Solid State Lasers and Synthetic Nonlinear Materials," revised in June 1986, was amended by correspondence on several occasions. A summary of the relevant correspondence appears in a letter from Marilynne Elverson and Robert L. Byer to Faye Coleman, dated 21 May 1987. Our discussion here details the reasons for deviations from the original equipment list. The equipment list divides naturally (according to intended use) into three sections as shown in parts IA & IB above.

### FTIR spectrometer and accessories

The first heading, FTIR spectrometer and accessories, reveals several important changes between the original proposal and the final purchases. Ben Yoo, a graduate student in the Byer research group, performed a careful evaluation of the best choice of FTIR instrument and accessories required for the research in quantum well synthetic nonlinear media. His conclusions led to the purchase of the group of accessories listed in part B above in place of the proposed IBM IR/32 FTIR Spectrometer System with Automated Microscopy. Many of the accessories required for the research had not yet been identified as essential when the original proposal was submitted. A discussion of the research made possible by the purchase of this equipment appears in parts III and IV. Note that the final price for the purchased system is within \$1345 of the original system cost.

### **Specific research instruments**

Under the heading of specific research instruments there are several important differences between the original proposal and the final purchases. Note especially that the price of the Quanta-Ray Nd:YAG laser ended up being \$59,500 instead of the anticipated \$48,000. The reasons for the change are twofold: 1) Spectra-Physics no longer produces the model of laser on which the original price estimate was based (Quanta-Ray DCR-2A(10)), and 2) research requirements not anticipated when the equipment was originally proposed made it necessary to buy a laser with a higher pulse repetition rate of 30 pulses per second instead of 10 pulses per second. The higher repetition rate of the purchased laser makes it possible to obtain data in an x-ray microscopy experiment three times as fast as the 10 pulses per second model would permit, an important consideration in a practical scanning microscopy system. Similar advantages accrue in experiments involving x-ray lithography and nonlinear optical frequency conversion.

To make up the \$11,500 difference in cost, the proposed \$11,500 Gaertner Research Spectrometer was deleted from the equipment list. These changes were explained in a letter dated 6 January 1987 from Marilynne Elverson to Faye Coleman.

The proposed \$34,600 HP 8568B RF Spectrum Analyzer was changed to a \$32,880 HP 71100A RF Spectrum Analyzer to take advantage of HP's new line of modular spectrum analyzers. The new spectrum analyzers perform as well as the old ones but offer cost savings and convenience.

The price of the pyroelectric vidicon and accessories rose from the original \$12,495 figure to \$13,595 while the contract was being considered.

### **Equipment for Optics Shop**

The main exception to the original proposal for optical shop equipment is the addition of the Emco coordinate milling and drilling machine. The apparatus is required for optical fabrication. It greatly expands the shop's ability to perform diamond grinding of crystals and lenses, including making angles, slots, concave and convex cylinders, spheres and flats. The request for the funds and the justification for the request were given in a letter dated 4 November 1986 from Marilynne Elverson and R. L. Byer to AFOSR Grant Officer.

Another important change is that the proposed Carl Zeiss Invertoscope M with various objectives for DIC interference was not purchased. Instead, we were able to find a surplus microscope that could be made suitable by buying appropriate accessories at a cost of \$9,014 instead of the anticipated \$20,000.

### III. SUMMARY OF RESEARCH PROJECTS INVOLVING EQUIPMENT PURCHASED UNDER THE GRANT

#### 1. FTIR Spectrometer and supporting equipment

##### a) Use of the FTIR for experiments on high critical temperature superconductors

A use of the FTIR that could not have been anticipated when the equipment was purchased is its application to measurements on thin films of Y-Ba-Cu-O high critical temperature superconductors. Ivan Bozovic, a visiting scientist working with Professors Geballe, Beasley, and Kapitulnik in the Ginzton Laboratory, has used the FTIR spectrophotometer and the Spectratech IR microscope to search for evidence of excitonic spectral resonances in the normal state of the thin films. These resonances are predicted to exist according to some models that attempt to explain the high critical temperature superconductors. No evidence for the existence of normal state excitonic spectral resonances has been found, which poses a severe challenge to the excitonic superconductivity models. A manuscript containing the experimental results has been submitted to Physical Review Letters. A copy of the manuscript is attached.

##### b) Special Circumstances regarding purchase of FTIR

Ben Yoo, a graduate student in Byer's group, made a careful and complete study of the available FTIR instruments before purchasing the Digilab FTS 40 system. His conclusion is that the purchased instrument has the best signal to noise ratio among the marketed devices. Several auxilliary pieces of equipment were purchased for use with the FTIR spectrometer.

- i) The MMR refrigerator was bought in order to cool GaAs quantum well samples during measurements with the FTIR
- ii) ZnSe windows from PTR were used on the MMR refrigerator system to admit infrared radiation to the cooled sample.
- iii) The Sargent-Welch vacuum pump is used in conjunction with the MMR refrigerator to improve its cooling capacity.
- iv) The InSb detector allows more sensitive measurements at 5 microns
- v) The wiregrid polarizers from PTR enable polarization sensitive measurements with the FTIR

Measurements made thus far with the FTIR system include the analysis of a 1% absorption in a GaAs quantum well sample cooled to 80K in the MMR refrigerator. The results will be

discussed at the OSA annual meeting in Rochester, NY, on October 19, 1987. The InSb detector used in the FTIR has improved the signal-to-noise ratio by a factor of 10 at the 5 micron wavelength compared to the HgCdTe detector normally used.

## 2. The Hewlett Packard RF Spectrum Analyzer

The RF spectrum analyzer has been used by many members of the research group. Santanu Basu, a graduate student in the Byer group, has used the spectrum analyzer to optimize a diode-pumped, mode-locked glass oscillator. The output of the laser is focused on a fast photodiode, and the spectrum analyzer receives the signal from the photodiode. The beat notes between the various axial modes running simultaneously in the laser cavity appear across the RF spectral region covered by the spectrum analyzer. Santanu has been able to verify when his laser is successfully mode-locked, optimize the mode-locking, and measure the amplitude and phase noise in the mode-locked output.

Alan Nilsson intends to use the RF spectrum analyzer to characterize the frequency stability of diode-pumped solid state lasers. In this application two diode-pumped, monolithic, nonplanar ring lasers have their outputs heterodyned on a photodetector, and the RF spectrum analyzer is used to measure spectral properties of the heterodyne signal. The broad spectral coverage of the HP RF spectrum analyzer make these measurements much simpler to carry out, and the narrow resolution the instrument offers allows meaningful measurement of extremely stable signals. A reprint of early measurements on nonplanar ring lasers is included. Note that one of the figures in the paper shows the use of an HP RF spectrum analyzer for frequency stability characterization.

## 3. Equipment for Optics Shop

Joe Vhrel of the Ginzton Laboratory Optics Shop specified the equipment to be purchased under this grant with the goal of upgrading the capabilities of the optics shop. The experience with the new equipment so far has been that more precise work is possible on both larger and smaller samples than could previously be worked on in the shops. The mills and lathes have enabled the optics shop to perform many custom machining tasks associated with mounting and preparing optics. The sphere generator is frequently used for applying spherical ends on miniature laser rods and other custom optics, as well as making possible the grinding of lenses. These tasks were previously performed by hand. The microscope makes possible a careful characterization of flatness, roughness, and optical quality of samples. The equipment purchased under the grant is used daily for tasks supporting many of the research groups in the Ginzton Laboratory.

#### 4. Nd:YAG LASER

The DCR3(30) Nd:YAG laser is in constant use for the X-ray microscopy experiments of John Trail. The pulsed output from the laser is focused onto a solid metal target in a vacuum chamber. The resulting laser produced plasma generates soft x-rays that are focused by normal incidence x-ray optics (Schwarzschild objective) to a small spot. John Trail has assembled most of the system already, and he recently reported his progress in a poster session at the Brookhaven National Laboratory Symposium on X-ray Microscopy.

Another application of the laser produced plasmas made possible by the Nd:YAG laser is the measurement of the reflectivities of multilayer x-ray mirrors. John Trail and others have measured the spectral reflectivities of such mirrors, and their results have been submitted to Applied Physics Letters. A copy of the manuscript is included in this report.

#### 5. CO<sub>2</sub> laser

The CO<sub>2</sub> laser is used primarily for second harmonic generation experiments involving synthetic nonlinear media. GaAs quantum well devices can be used to generate the second harmonic of the nominally 10 micron radiation from the CO<sub>2</sub> laser. Fabrication of appropriate GaAs structures is in progress.

### IV. SYNOPSIS OF RESEARCH ACTIVITIES OF THE BYER GROUP

Included below is a list of the members of Professor Byer's research group as of Autumn 1987. The list serves as a concise summary of the research activities currently being pursued in the group. A more detailed description of some of the research interests appeared in the original proposal "Tunable Solid State Lasers and Synthetic Nonlinear Materials."

BYER GROUP - 1987/1988

Robert L. Byer - Principal Investigator  
 Robert Eckardt - Senior Research Associate  
 Martin Fejer - Acting Assistant Professor  
 Eric Gustafson - Research Associate  
 Mary Farley - Group Secretary

SLAB GEOMETRY LASERS

10 J, 10 Hz Fixed Slab Glass Laser Source  
 Moving Glass Slab Laser Source

Murray Reed  
 Santanu Basu

LASER PLASMA SOFT X-RAY STUDIES

Picosecond Source for X-ray Lithography  
 Soft X-ray Microscope

Santanu Basu  
 John Trail

SINGLE CRYSTAL FIBER STUDIES

Harmonic Generation in LiNbO<sub>3</sub> Fibers  
 Quasi-Phasematching in LiNbO<sub>3</sub> Fibers  
 Parametric Generation in Crystal Fibers  
 Propagation in Birefringent Fibers

Greg Magel  
 Greg Magel  
 Dieter Jundt  
 Mei Lu

DIODE LASER PUMPED SOLID STATE LASERS

LiNbO<sub>3</sub> Optical Parametric Oscillator Studies  
 Diode Laser Pumped Nonplanar Ring Oscillator Linewidth Studies  
 Harmonic Generation for Squeezed States

Bill Kozlovsky  
 Alan Nilsson  
 David Nabors

NONLINEAR MATERIALS

AgGaSe<sub>2</sub> Infrared Parametric Oscillator  
 Second Harmonic Generation of CO<sub>2</sub> Laser  
 AgGaS<sub>2</sub> Infrared Parametric Oscillator

Robert Eckardt  
 Robert Eckardt  
 Y. X. Fan

SYNTHETIC NONLINEAR MATERIALS

Quantum Well GaAs Nonlinear Media Studies  
 Quasi-Phasematching in Guided Wave Structures  
 Medical Applications of Lasers

Martin Fejer  
 Eric Lim, Ben Yoo  
 Scott Layne

VISITORS

Dr. J. Unternahrer  
  
 K. Maeda

Hoya Optics, Inc.,  
 Japan  
 Sumitomo Metal &  
 Mining Co., Japan

**V) SUMMARY**

This report has given a final accounting of the use of Equipment Grant AFOSR-86-0275 to finance equipment useful in both daily laboratory applications and in specific areas of research. The AFOSR equipment grant has helped us to replace outdated equipment in the Optics Shop and to expand our research capabilities considerably through the purchase of new lasers, the FTIR spectrophotometer and its accessories, and the RF spectrum analyzer. New research avenues are already opening, as the included manuscripts show. We are grateful to the AFOSR for making these purchases possible.

**Enclosures:**

- 1) Manuscript of paper by Bozovic et al., submitted to Physical Review Letters regarding measurements of properties of thin film, high critical temperature superconductors
- 2) Abstract of results of Yoo et al. on properties of GaAs quantum well structures, to be presented at OSA conference in October, 1987
- 3) Abstract of Soft X-ray Microscope results of John Trail, presented at Brookhaven National Laboratory in September, 1987
- 4) Manuscript of paper submitted to Applied Physics Letters, reporting the measurement of x-ray multilayer mirror characteristics by Trail et al.
- 5) Reprint of Optics Letters paper by Kane et al. on frequency stability of diode-pumped nonplanar ring lasers

Submitted to Phys. Rev. Lett  
Aug 23, 1987

**OPTICAL MEASUREMENTS ON ORIENTED THIN  $\text{YBa}_2\text{Cu}_3\text{O}_{7-\delta}$  FILMS: LACK OF EVIDENCE FOR EXCITONIC SUPERCONDUCTIVITY**

by

I. Bozovic<sup>a</sup>, D. Kirillov<sup>b</sup>, A. Kapitulnik<sup>a</sup>, K. Char<sup>a</sup>, M.R. Hahn<sup>a</sup>, M. R. Beasley<sup>a</sup>, T. H. Geballe<sup>a</sup>, Y.H. Kim<sup>c</sup> and A. J. Heeger<sup>c</sup>

a) Department of Applied Physics, Stanford University, Stanford, CA 94305-4090.

b) Varian Research Center, Palo Alto, CA 94303.

c) Department of Physics, University of California, Santa Barbara, CA 93106.

**ABSTRACT**

Optical transmission and reflection spectra (mid IR through UV) and Raman spectra of superior quality 90 nm, 180 nm, 400 nm and 1000 nm thick superconducting Y-Ba-Cu-O films are reported. Characteristic excitonic bands, and in particular the absorption band at  $\sim 0.37\text{eV}$  reported earlier, are not observed. It therefore seems unlikely that the high- $T_c$  superconductivity in cuprates could arise from exciton-mediated electron pairing.

PACS NO. 74.70

The discovery of high- $T_c$  superconductivity in cuprates<sup>1</sup> has stimulated unprecedented research activity. Much of the effort is focussed on understanding the underlying mechanism of the superconductivity, and a number of models have already been proposed<sup>2-4</sup>. Some of them are specific enough to be directly tested experimentally. However, the usually most powerful technique for identifying the mechanism, the tunneling spectroscopy, has been greatly hampered so far by generally bad quality of the surface of oxygen-annealed cuprate pellets and films. Infrared spectroscopy probes much deeper into the bulk of the sample and thus could play an important role in clarifying the mechanism of superconductivity in these materials.

The optical reflectivity spectra of La-Sr-Cu-O and Y-Ba-Cu-O have been measured<sup>5-7</sup> over a broad frequency range (far IR through UV). However, since reflectivity depends both on the real and the imaginary part of the dielectric function, such spectra cannot be interpreted directly in general. Orenstein et al.<sup>5</sup> tried to fit their data by the simple classical Drude model:  $\epsilon(\omega) = \epsilon(\infty) - \omega_p^2 / \omega(\omega + i\Gamma)$ ; their optimal parameter values were  $\omega_p = 2\text{eV}$  and  $3\text{eV}$  for La-Sr-Cu-O and Y-Ba-Cu-O respectively, and  $\Gamma = 0.5\text{ eV}$  and  $\epsilon(\infty) = 4.5$  for both compounds. The calculated reflectivity turned out to be much too large in the mid-IR and near-IR region (0.1 eV to 1 eV). Orenstein et al.<sup>5</sup> concluded that an optically allowed transition across a gap occurs at  $\sim 0.5\text{ eV}$  in La-Ba-Cu-O; a similar result was obtained for Y-Ba-Cu-O. Therefore, they inferred that the corresponding strong absorption band (with the peak absorption coefficient of  $\sim 10^5\text{cm}^{-1}$ ) should be directly observable in transmission experiments on thin films. Finally, they found this IR feature to be absent in undoped  $\text{La}_2\text{CuO}_4$ , thus tying it to superconductivity. Etemad et al.<sup>5</sup> also found the correlation between the occurrence of the 0.5eV peak and superconductivity in  $\text{La}_{2-x}\text{Sr}_x\text{CuO}_4$ . Kamaras et al.<sup>6</sup>, by an analogous methodology, concluded that two strong electronic transitions occur at 0.44 eV and 1.3 eV in La-Ba-Cu-O, and at 0.37 eV and 2.5 eV in Y-Ba-Cu-O. In oxygen-depleted (non-superconducting)  $\text{YBa}_2\text{Cu}_3\text{O}_{6.2}$  samples, the 0.37 eV peak was absent. They interpreted these spectral features as the charge-transfer-exciton bands, in

support of the excitonic superconductivity model of Varma et al.<sup>2</sup>. Finally, Schlessinger et al.<sup>7</sup> also recorded similar spectra but derived just the opposite conclusion. Inspired by the recent report<sup>8</sup> of single-crystal  $\text{La}_2\text{NiO}_4$  reflectivity spectra, which show extremely anisotropic (quasi-two-dimensional) character, they concluded that no extra interband transition has to be postulated if  $\text{La}_2\text{CuO}_4$  has similar anisotropy.

The above controversy - important in view of its implications concerning the pairing mechanism in the cuprate superconductors - can be resolved by a direct IR transmission measurement. The principal difficulty here comes from the short light penetration depth of these materials that imposes nontrivial requirements on sample preparation. Synthesis of thin Y-Ba-Cu-O films on various substrates has been reported by the Stanford thin films group and subsequently by several other groups<sup>9</sup>. Sharp (2 K wide) transitions with  $T_c$  above 90 K, and high critical currents of over  $2.0 \times 10^6$  A/cm<sup>2</sup> (at 4.2 K) have been achieved. Typical thicknesses of these films were about 1  $\mu\text{m}$ ; such films are not transparent in the IR region. The same is true for the usual powdered Y-Ba-Cu-O ceramics with typical particle size of 1-10  $\mu\text{m}$ .

With this motivation, we have synthesized a series of 90 nm, 180 nm, 400 nm, and 1000 nm thick superconducting Y-Ba-Cu-O films of various orientations, on  $\text{SrTiO}_3$  substrates, using the reactive-magnetron-sputtering technique. A detailed description of the preparation and characterization method is given elsewhere<sup>10</sup>. X-ray diffraction shows a highly crystalline, single-phase, homogeneous and highly-oriented material. The films are optically semitransparent, uniform and homogeneous. Resistivity measurements show extremely sharp ( $\sim 1.5$  K total onset-to-zeroresistance width) superconducting transitions at  $T_c = 90$  K typically. Magnetization measurements show critical current densities in excess of  $1.2 \times 10^7$  A/cm<sup>2</sup> at 4.2 K and  $6 \times 10^5$  A/cm<sup>2</sup> at 78 K (for the films with the c axis oriented perpendicular to the film surface). Measurements of the angular dependence of the magnetization loops (as discussed in Ref. 10) showed a surface barrier of  $\sim 10$  kG, indicating a surface current density of  $3 \times 10^8$  A/cm<sup>2</sup>, the

highest reported so far . Typical resistivity of these films in the normal state is given by:  $\rho \approx 1.2 \text{ T} + 15 \mu\Omega\text{-cm}$  , the lowest reported for these materials. The above results suggest that the films investigated were of much improved quality.

Using these films, we have recorded reflectance and transmittance spectra and Raman spectra over a broad range of frequencies and at temperatures ranging from 10K to 300K. The infrared transmittance and reflectance measurements were made on a Biorad FTS-40 FTIR spectrophotometer coupled with a Spectratech IR microscope, and an IBM 98 (Bruker) FTIR interferometer. For the Raman scattering experiment an  $\text{Ar}^+$  ion laser, a Spex triple scanning monochromator and a cooled GaAs photomultiplier detector were utilized. The same monochromator and detector, as well as a Varian-Cary double-beam spectrophotometer, were utilized to record the near-IR through UV transmittance spectra.

The first observation is that our films show much higher mid-IR specular reflectance than the ceramic samples of Refs. 5-6, in fact, higher than the Drude-model fit of Orenstein et al.<sup>5</sup> In Fig. 1 we show our reflectance data of a polycrystalline film together with the data of Refs. 5 and 6. No extra absorption peak at  $\sim 0.4 \text{ eV}$  is inferred from the data. This reflectance spectrum can well be fitted by a simple Drude model, with:  $\omega_p = 2.6 \text{ eV}$  ,  $\Gamma = 0.65 \text{ eV}$  and  $\epsilon(\infty) = 4.5$

An independent and direct proof of this conclusion comes from the transmittance spectra of the films which are featureless in this frequency range (see inset of Fig.1.) All other samples of comparable quality - over a dozen films, of various orientations - showed similar spectra. Note the transmittance and reflectance of the 90 nm film which indicate a substantial absorption background.

The Raman spectra of these films also show an electronic background which is featureless , see Fig.2. Finally, no peaks emerged in either the IR or the Raman spectra at lower temperatures, down to 10 K (scanning densely the region around  $T_c$ ).

The absence of excitonic resonances in our IR and Raman spectra still leaves a remote

possibility that an excitonic transition exists, but it is neither dipole nor quadrupole allowed. In more detail, the space group of  $\text{YBa}_2\text{Cu}_3\text{O}_7$  is  $D_{2h}^4$  (Pmmm), and the maximal site symmetry (enjoyed by Cu(1) and O(1) atoms) is  $D_{2h}$ . This group does have one "silent" (i.e. optically inactive) irreducible representation,  $A_u$  - the one that is odd with respect to each of the three symmetry planes ab, ac, and bc. However, to within a few eV above  $E_F$ , in  $\text{YBa}_2\text{Cu}_3\text{O}_7$  there are no transitions that reverse the parity with respect to each of these three mirror planes. Moreover, to be relevant for superconductivity, the excitons have to be mobile, but any dispersion would make direct ( $\Delta k=0$ ) transitions into all but few (Brillouin-zone center and edge) excitonic states IR and/or Raman allowed.

Therefore, it seems that in  $\text{YBa}_2\text{Cu}_3\text{O}_7$  there are no excitons close to the Fermi level, which are assumed to be necessary<sup>3</sup> for excitonic superconductivity. In fact, we have recorded the transmittance spectra of  $\text{YBa}_2\text{Cu}_3\text{O}_7$  films from mid-IR through UV (0.1 eV to 3.5 eV), and observed no sharp absorption peaks typical of excitonic states ( Fig. 3) . Hence, we believe that excitons - at least in the usual sense of Frenkel excitons, charge-transfer excitons<sup>2</sup> or Wannier-Mott excitons - are not formed in our superconducting  $\text{YBa}_2\text{Cu}_3\text{O}_7$  samples. This should not be surprising, in view of their high conductivity, approaching that of Bi or Hg.

It may be interesting to note that some of the films prepared earlier, which had somewhat inferior superconducting characteristics (broader transitions, smaller critical currents, less homogeneity) did show a broad absorption feature in the IR measurements centered at about 2500 - 3000  $\text{cm}^{-1}$  (0.3 - 0.4 eV) with a similar feature in the Raman spectrum. However, this feature is not nearly as pronounced as was concluded in Refs. 5 and 6. This band is very broad, in contrast to usually rather narrow excitonic features. Both the strong Raman peak and the weak IR feature are seen at room temperature and show little temperature dependence. Thus it seems that this electronic transition is not characteristic of the high- $T_c$  superconducting material, but rather of some structurally or compositionally disordered regions in less homogeneous samples. The important

point that we stress here is that good superconducting films exist without any trace of the 3000  $\text{cm}^{-1}$  IR band.

In conclusion, we have prepared superconducting Y-Ba-Cu-O films thin enough to enable high-quality mid-IR through UV absorption measurements. In contrast to some earlier reflectivity studies<sup>5,6</sup>, no spectroscopic features suggestive of excitonic absorption are seen. It thus seems unlikely that the observed high- $T_c$  superconductivity in Y-Ba-Cu-O originates from exciton-mediated electron pairing. Moreover, no other sharp bosonic excitations (e.g. magnons) are detected either. Strong but featureless absorption we observed is more suggestive of fermions (e.g. polarons) - perhaps quasi-localized in view of the interband-transition-edge smearing which does not change much from room temperature down to 10 K. Also the large damping and the low Hall-mobility ( $\sim 8 \text{ cm}^2/\text{V}\cdot\text{s}$  for good c-axis films) that we have measured on these films.

**Acknowledgement :**

We are grateful to C. Herring and S. Doniach for useful discussions and to J. McDevitt. This research was supported by the AFOSR, the ONR and the NSF through grants of the individual researchers. Materials were prepared and characterized at the Center for Materials Research, at Stanford University.

## REFERENCES:

1. J. G. Bednorz and K. A. Müller, Z. Phys. B. 64, 189 (1986); M. K. Wu et al., Phys. Rev. Lett. **58**, 908 (1987).
2. C. Varma et al., Solid State Commun. **62**, 681 (1987).
3. W. A. Little, Proc. Int. Workshop on Novel Mechanisms of Superconductivity, June 22-26, 1987, Berkeley, CA; J. Bardeen et al., *ibid*; J. Yu et al., *ibid*.
4. P.W. Anderson, Science **235**, 1196 (1987);  
S. Kivelson et al., Phys. Rev. **B35**, 8865 (1987);  
D. Pines, in Ref. 3; S. Doniach, *ibid* :  
V. Kresin, Phys. Rev. **B35**, 8716 (1987);  
J. Ruvalds, Phys. Rev. **B35**, 8869(1987);  
V.J. Emery, Phys. Rev. Lett. **58**, 2794 (1987);  
P.G. deGennes, preprint.
5. J. Orenstein et al., Phys. Rev. **B36**, 729 (1987);  
S. Etemad et al., preprint.
6. K. Kamaras et al., Phys. Rev. Lett. **59**,919 (1987); S. L. Herr et al., Phys. Rev. **B36**, 733 (1987).
7. Z. Schlessinger et al., Proc. Int. Workshop on Novel Mechanisms of Superconductivity,

June 22-26, 1987, Berkeley, CA.

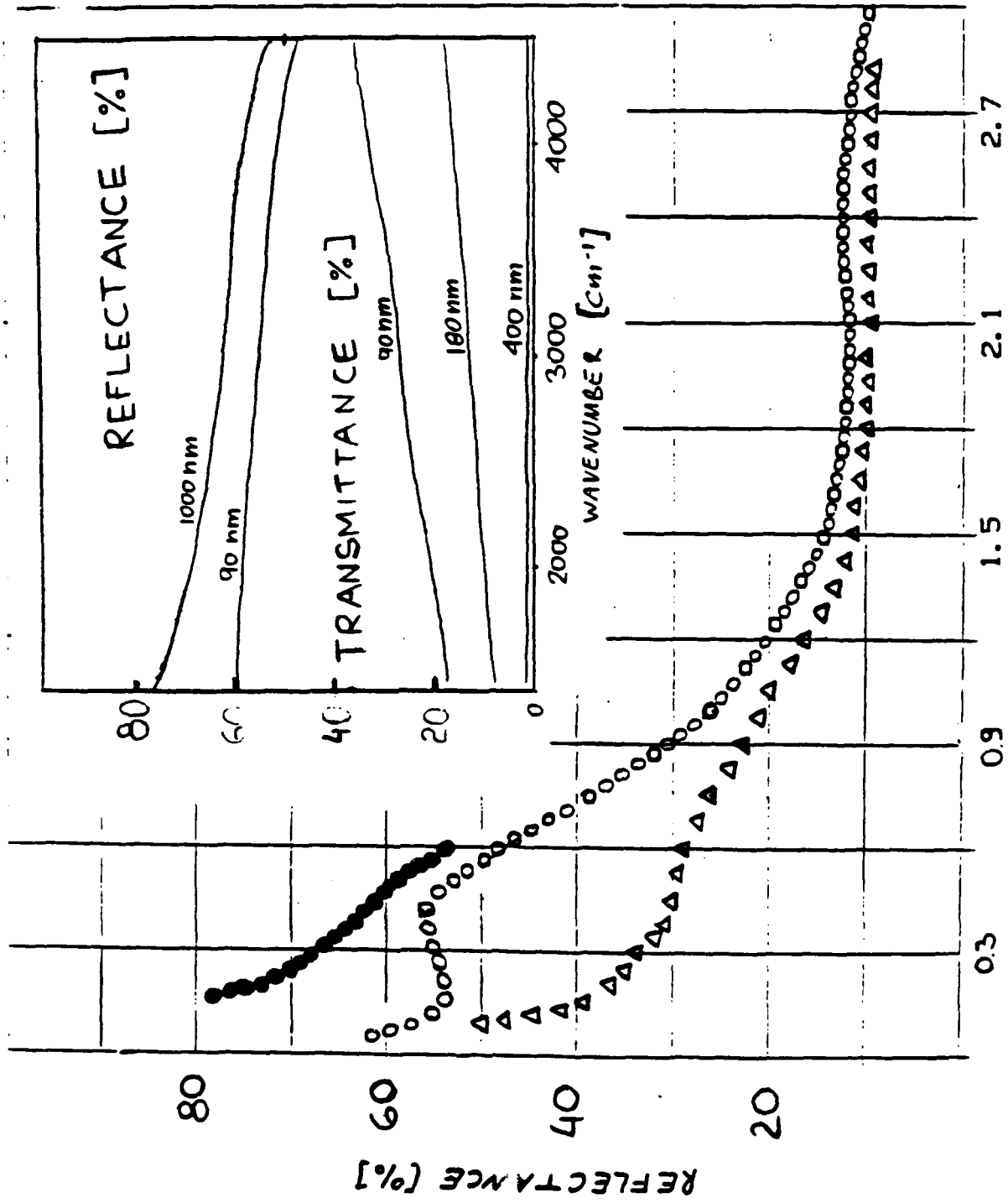
8. J. M. Bassat et al., Phys. Rev. **B35**, 7126 (1987).
9. A. Kapitulnik et al., Proc. Int. Conf. on High-Tc Superconductivity, ICTP, Trieste, July, 1987, World Scientific Publishing Inc.
10. K. Char et al. Appl. Phys. Lett., in press;  
B. Oh, et al. Appl. Phys. Lett., in press.

## FIGURE CAPTIONS

**Fig. 1:** Reflectance from randomly-oriented 1 $\mu$ m thick film (o), compared to bulk-ceramic data of Ref.5 (o) and Ref.6 ( $\Delta$ ). Inset : mid-IR reflectance (upper two curves) and transmittance (lower three curves) of films with various thicknesses.

**Fig. 2:** Raman scattering (at 300 K) from a good superconducting film (400 nm thick, a-axis oriented) .

**Fig. 3:** IR to UV transmittance spectrum of the film C (180 nm, c-axis oriented) . Inset shows the interband transition edge on an expanded scale.



ENERGY [eV]

Fig. 1

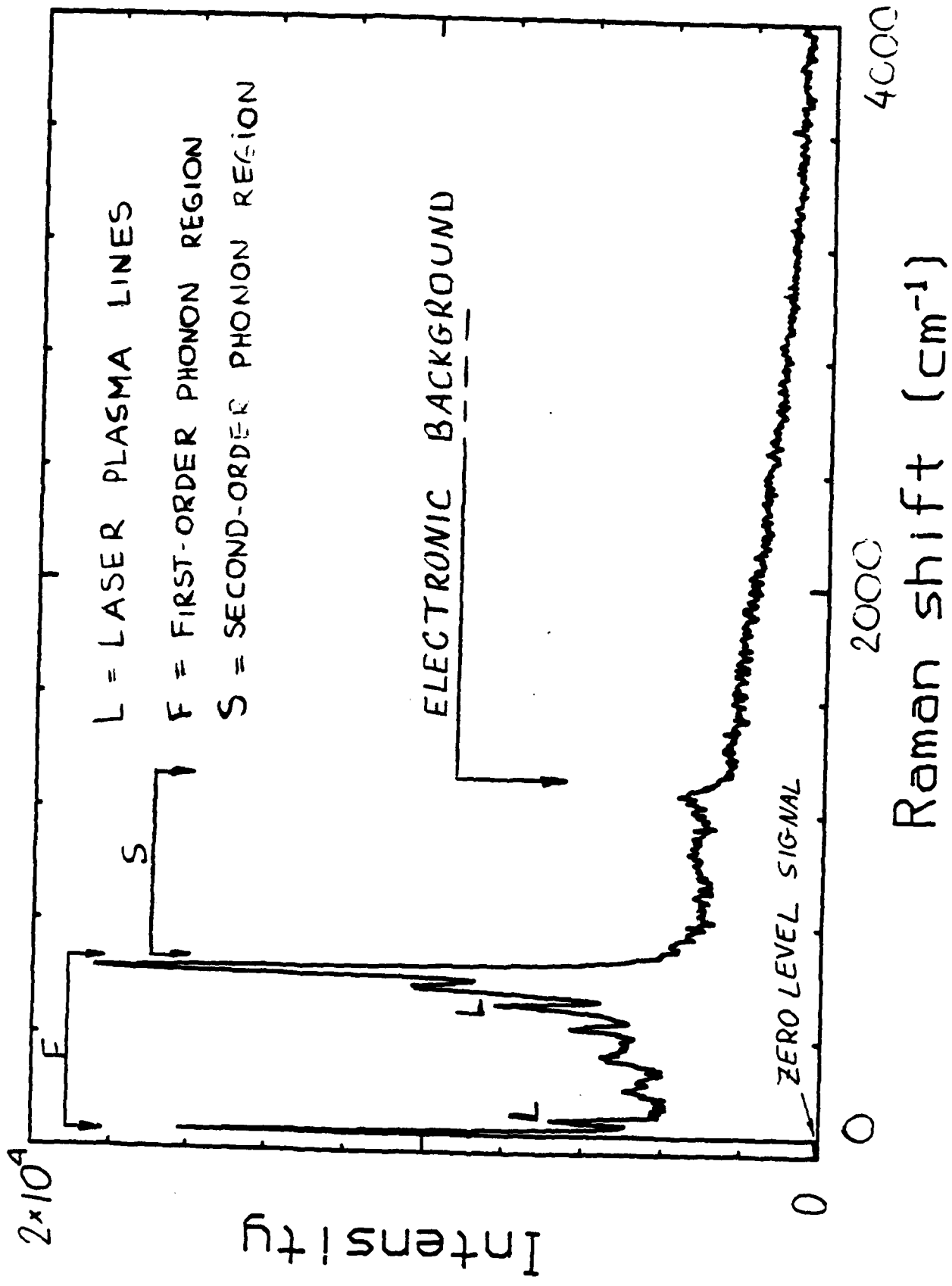


Fig. 2.

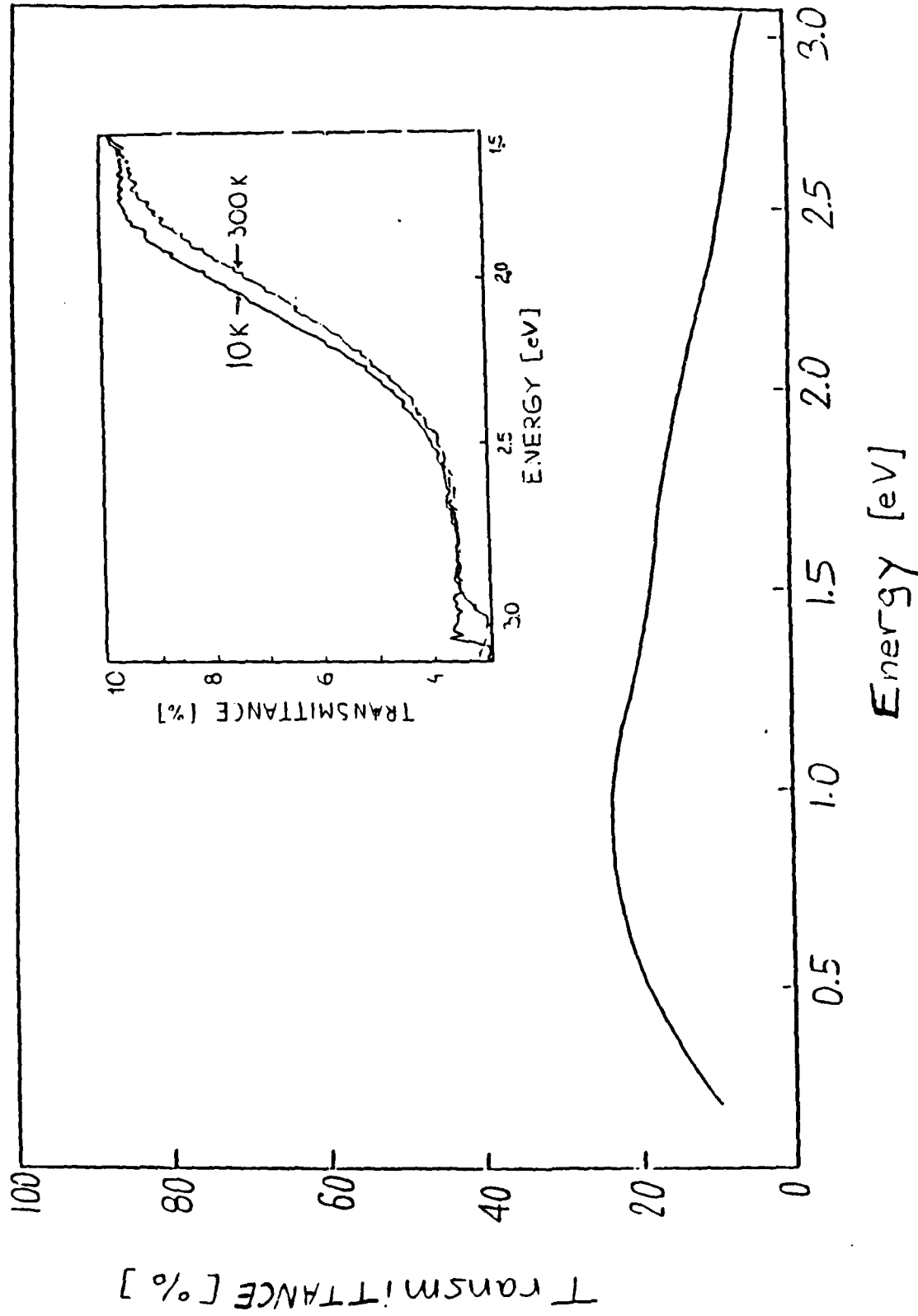


Fig. 3

submitted to OSA  
'87

Second Harmonic Generation in DC-Biased Quantum Wells

S. J. B. Yoo, M. M. Fejer, Alex Harwit, R. L. Byer, and J. S. Harris, Jr

ABSTRACT

DC-biased quantum wells possess large quadratic nonlinear susceptibilities, whose sign and magnitude are controlled by the applied field. Experimental and theoretical results for second harmonic generation are discussed.

It has recently been shown that the dipole matrix elements between subbands in semiconductor quantum wells are extremely large.<sup>1</sup> Third order nonlinear susceptibilities are proportional to the fourth power of these matrix elements. Large nonlinearities have thus been predicted for these systems, in particular an intensity dependent index of refraction suitable for use in all-optical logic elements.<sup>1</sup> Second order nonlinearities vanish identically in symmetric wells, suggesting the use of asymmetrically graded quantum wells for quadratic interactions.<sup>2</sup> External bias electric fields also break the inversion symmetry, resulting in Stark shifts, and large quadratic susceptibilities whose sign depends on the direction of the applied field. The magnitude of the nonlinearity depends on the carrier density, the DC bias field, and the detuning of the fundamental and second harmonic frequencies from resonances. For reasonable experimental parameters, and sufficient detuning to minimize linear absorption, theoretical predictions suggest that nonlinear susceptibilities an order of magnitude larger than bulk GaAs are possible. Efficient nonlinear optical devices require phasematching as well as a large nonlinear susceptibility. A periodic electrode structure for the bias fields leads to a periodic variation in the sign of the nonlinear susceptibility, which can be used to quasiphase-match the interaction. This control over nonlinear susceptibility and absorption, and the elimination of phasematching constraints, make DC-biased quantum wells an attractive synthetic nonlinear medium for infrared interactions. Preliminary measurements of frequency doubling of the 10.6  $\mu\text{m}$  output of a  $\text{CO}_2$  laser incident at Brewster's angle on a substrate with 50 DC-biased AlGaAs/GaAs quantum wells indicate that the nonlinear susceptibility is of the same order of magnitude as theoretical predictions. Progress in these measurements will be reported, and waveguide device configurations for efficient nonlinear interactions described.

\* Stanford Electronics Laboratory

---

<sup>1</sup> L. C. West and S. J. Eglash, Appl. Phys. Lett. 46, 1156 (1985).

<sup>2</sup> M. K. Gurnick and T. A. DeTemple, IEEE J. Quantum Electron. QE-19, 791 (1983).

P R O G R A M

---

International Symposium on X-Ray Microscopy

August 31 - September 4, 1987

Brookhaven National Laboratory  
Physics Building - 510

Sponsors:

National Synchrotron Light Source, Brookhaven National Laboratory

National Science Foundation

Physics Department, SUNY at Stony Brook

Center for X-Ray Optics, Lawrence Berkeley Laboratory

- Scanning Photoemission Microscope at XI  
H. Ade, J. Kirz, H. Rarback, S. Hulbert, D. Kern and Y. Vladimirovsky
- X-Ray Microscopy Studies on the Pharmacodynamics of Therapeutic Gallium in Rat Bones  
R. Bockman, M. Repo, R. Warrell, J.G. Pounds, W.M. Kwiatak, G.J. Long, G. Schidlovsky and K.W. Jones
- Design for a Fourier-Transform Holographic Microscope  
K. Boyer, D. Cullen, W.S. Haddad, C.K. Rhodes, J.C. Solem and R.S. Weinstein
- Initial Location of Gold Sites in Carlin-Type Ores Using Synchrotron X-Ray Microscopy  
J.R. Chen, E.C.T. Chao, J.A. Minkin, J.M. Back, W.C. Bagby, A.L. Hanson, K.W. Jones, M.L. Rivers and S.R. Sutton
- Exploration of Demyelinated Axon of Medulated Shrimp Nerve by Soft X-Ray Microscopy  
S.-F. Fan, H. Rarback, H. Ade and J. Kirz
- Comparison of Soft X-Ray Contact Microscopy with Other Microscopical Techniques for the Study of the Fine Structure of Plant Cells  
T.W. Ford, A.D. Stead, W. Myring, C. Hills and R. Rosser
- Biological Applications at LBL's Soft X-Ray Contact Microscopy Station  
G.D. Guttman and M.R. Howells
- X-Ray Microscopy of Single Neurons in the Central Nervous System  
J.E. Hamos
- Photo-Resist Studies on X-Ray Contact Microscopy  
G.-J. Jan, L.F. Chen, Y.J. Twu and D.C. Hung
- Imaging X-Ray Microscopy with Extended Depth of Focus by Use of a Digital Image Processing System  
L. Jochum
- A Zone Plate Soft X-Ray Microscope Using Undulator Radiation at the Photon Factory  
S. Kagoshima, S. Aoki, M. Kakuchi, M. Sekimoto, H. Maezawa, K. Hyodo and M. Ando
- Scanning X-Ray Microradiography and Related Analysis in an SEM  
D. Mouze and J. Cazaux
- Image Capture Possibilities with the Projection Shadow X-Ray Microscope  
S.P. Newberry
- Absorption Edge Imaging of Sporocide-Treated and Non-Treated Bacterial Spores  
B. Panessa-Warren, G. Tortora and J. Warren
- The Role of High Energy Synchrotron Radiation in Biomedical Trace Element Research  
J.G. Pounds, G.J. Long, W.M. Kwiatak, K.W. Jones, B.M. Gordon and A.L. Hanson
- X-Ray Contact Microscopy of Biological Specimens with Undulator Radiation  
K. Shinohara, H. Nakano, M. Watanabe, Y. Kinjo, S. Kikuchi, Y. Kagoshima, K. Kobayashi and H. Maezawa
- Soft X-Ray Contact Microscopy of Botanical Material Using Laser-Produced Plasmas or Synchrotron Radiation  
A.D. Stead, T.W. Ford, R. Eason, A.G. Michette, W. Myring and R. Rosser
- Advances in Geochemistry and Cosmochemistry: Trace Element Microdistributions with the Synchrotron X-Ray Fluorescence Microprobe  
S.R. Sutton, M.L. Rivers, and J.V. Smith
- The Stanford Scanning X-Ray Microscope  
J.A. Trail and R.L. Byer
- SEM Examination of X-Ray Microradiographs Formed on Uncoated Photoresist with a Low Loss Electron (LLE) Detector  
O.S. Wells and P.C. Cheng
- Contact Soft X-Ray Microscopy at Hefei  
X.-S. Kei, X.-Z. Jia, J. Ren, T. Jin and H.-J. Shen
- A Projection X-Ray Microscope Converted from a Scanning Electron Microscope and its Applications  
K. Yada and S. Takahashi

## **The Stanford Scanning X-ray Microscope**

**J.A. Trail and R.L. Byer  
Stanford University**

**T.W. Barbee Jr.  
Lawrence Livermore National Laboratory**

### **Abstract**

We describe our design and fabrication of a scanning X-ray microscope which uses normal incidence multilayer coated mirrors as the focussing elements and a laser-produced plasma as the source of soft X-rays. The microscope is compact with both the laser and the microscope fitting on a single optical table. We will present results of initial imaging tests of the microscope operating at a wavelength of  $140\text{\AA}$ .

**Measurement of Soft X-Ray Multilayer Mirror Reflectance  
at Normal Incidence using Laser-Produced Plasmas**

J.A. Trail and R.L. Byer  
Department of Applied Physics  
Stanford University

T.W. Barbee Jr.  
Chemistry and Materials Science  
Lawrence Livermore National Laboratory

Abstract

We have used Laser-Produced Plasmas as a broadband source of soft X-rays to measure the normal incidence reflectance of multilayer mirrors in the 10nm to 25nm spectral region. The measurements have a spectral resolution of 0.03nm and a reflectance resolution of 10%. Measurements made on a Mo/Si multilayer show excellent agreement with results obtained using a synchrotron and indicate a normal incidence peak reflectance of over 50% at 15nm. By repeating the reflectance measurement at different positions across a single 7.5cm mirror we determined multilayer uniformity as a function of position and we relate this dependence to the geometry of the deposition process. Aluminum filter transmission across the Al  $L_{2,3}$  edge was also measured.

The Laser-Produced Plasma is a bright, laboratory scale source of broadband radiation in the soft X-ray regime (1nm-30nm). This compact continuum source together with a grazing incidence monochromator makes an excellent tool for quickly and accurately measuring the performance of multilayer mirrors and transmission filters in the soft X-ray regime. In this letter we present experimental results that demonstrate the high spectral, amplitude and spatial resolutions of this measurement technique. By comparing with synchrotron results we also demonstrate the absolute accuracy of the technique.

In recent years there has been increasing use of multilayer structures<sup>1,2</sup> as narrowband reflectors in the X-ray (0.01nm - 1nm) and soft X-ray regimes. Multilayers are now routinely used as narrowband filters at near grazing angles<sup>3</sup> and more recently have been used as elements in a tunable monochromator at angles of incidence up to 56° off grazing<sup>4</sup>. Efforts are continuing on soft x-ray telescopes<sup>5,6</sup> and soft x-ray microscopes<sup>7,8</sup> both of which use multilayer mirrors at near normal angles of incidence. The multilayers used in these applications are usually required to have specific properties, i.e. the reflectance peak must be at a particular wavelength with specific requirements on peak reflectance and bandwidth. Confirming and improving the performance of multilayers requires accurate and prompt measurements of the fabricated multilayer properties.

Present measurements of multilayers are made using either stationary anode or synchrotron X-ray sources. The stationary anode X-ray source is a compact and readily available laboratory instrument. However, its emission is predominantly line emission concentrated above 250eV. The discrete nature of the X-ray emission limits multilayer testing with a stationary anode to rocking curve measurements, i.e. reflectance as a function of incident angle, at wavelengths and angles which are not necessarily near those of the intended application. Extrapolating the results to the conditions of the final application is often difficult due to the wavelength dependence of the multilayer material indices. The synchrotron source has been used to characterize multilayers both with rocking curves and with measurements in which angle of incidence is fixed and wavelength varied. The wide

tunability of the source allows measurements to be made at arbitrary wavelength and angle. However, synchrotrons have not been readily accessible or easily adapted to reflectance measurements.

A third source of soft X-rays, not previously used to measure multilayer reflectance, is the laser-produced plasma (LPP)<sup>9</sup>. By focusing a high peak power laser pulse onto a sufficiently dense material a plasma is formed which emits radiation across the soft X-ray region and into the X-ray region. The conversion efficiency from laser radiation to broadband soft X-rays can be high, routinely from 10% to 50%<sup>10</sup>, and for many target materials the emission spectrum is a continuum with minimal or no line structure<sup>11,12,13</sup>. The LPP source combines the advantages of bright continuum emission with the accessibility of a laboratory instrument.

In our measurements the LPP is formed by focusing pulses of 1064nm radiation from a Q-switched Quanta Ray DCR II Nd:YAG laser onto a solid copper cylinder located inside a vacuum chamber. The laser operates at 10Hz with a pulse length of 8ns and pulse energies of up to 800 mJ. For reflectance measurements near 15nm we require laser energies of only 10mJ per pulse. With a focal spot diameter of 30 $\mu$  the resulting intensity on the copper target is  $4.4 \times 10^{10} \text{ W cm}^{-2}$ . The target is rotated on a 40 pitch threaded rod to produce a clean area of target for each shot, aiding in the shot to shot reproducibility of the plasma and the soft X-ray emission.

A 1.5 meter grazing incidence grating monochromator mounted with a fast (1ns rise time) microchannel plate detector (MCP) is used to make spectral measurements in the soft X-ray regime. The monochromator is operated with a 1200g/mm grating and a 300 $\mu$  slit width with a concomitant resolution of 1.7 $\text{\AA}$ . The 300 $\mu$  slit width results in reasonable signal levels given the low X-ray intensities we use in order to avoid saturating the MCP detector. The signal from the detector is processed by a boxcar integrator then stored on a personal computer.

Figure 1 shows the experimental arrangement for measuring multilayer reflectance. The reflectance is obtained from two measurements over the same wavelength range. The first scan measures the direct plasma emission in the spectral region of interest for the particular multilayer and angle of incidence, and is made with the target in position (a). The second scan measures the plasma emission after reflection from the multilayer. The reflection is obtained by moving the target back several millimeters to position (b). Each scan takes from 2 to 5 minutes depending on the scan range, resolution and signal averaging. The area of reflection on the multilayer is determined by the size of the plasma source and the acceptance aperture of the monochromator. The X-ray emitting area of the plasma is small, measured to be  $100\mu$  in diameter, resulting in an area of reflection on the multilayer only  $200\mu$  wide by  $700\mu$  high.

With  $300\mu$  slit widths on the monochromator the 10mJ laser pulse results in an estimated 10,000 photons arriving at the MCP in the 8ns pulse at 15nm. The detector is shot noise limited resulting in an rms shot to shot signal variation of 1% for the direct scans and 3% for the reflected scans. Stability of the signal over several minutes is at present limited by instability in the position of the copper target. At present near-consecutive scans are reproducible to within 10% of the absolute value. Future improvements in target design and in repeatable target positioning should improve the reproducibility of the results.

Figure 2 shows both the direct plasma spectrum for a copper target from 13nm to 17nm and the spectrum reflected off a Mo/Si multilayer<sup>14</sup> oriented at 0.8 degrees from normal incidence. The reflected spectrum shown has been corrected for the change in optical path length in going from a direct scan to a reflected scan. The multilayer consists of 62 layer pairs with a pair thickness of 7.9nm deposited on a 2.5cm diameter super-polished glass substrate. This substrate has an rms surface roughness of less than 0.3nm and a figure quality of 0.05 wave at 633nm.

The multilayer reflectance is obtained by dividing the corrected reflected plasma scan by the direct plasma scan. Figure 3 shows the reflectance curve obtained for the Mo/Si

multilayer described above and a synchrotron measurement of the same multilayer<sup>15</sup>. The LPP and synchrotron reflectance measurements are in excellent agreement. Further, the experimental results agree very well with theory which predicts a peak normal incidence reflectivity of 57% with a 0.7nm bandwidth.

For all applications of multilayers it is important to know the variation of the multilayer period across the coated wafer or optic. This is particularly true for normal incidence imaging applications which often require large reflecting areas with specific filtering properties. By mounting the multilayer on a translation stage inside the vacuum chamber it is a simple matter to move the area of reflection between scans and make detailed reflectance measurements across the full extent of the multilayer. At normal incidence the small 200 $\mu$  by 700 $\mu$  area of the reflection makes this very close to a point measurement technique.

Figure 4 shows the results of measurements made at several points on a single Mo/Si multilayer. The multilayer consists of 20 layer pairs with a pair thickness of 9.35nm deposited on a 7.5cm diameter polished silicon wafer. In the deposition process the substrate is mounted in an inverted position on a table which rotates above magnetron sputtering sources. The center of the wafer substrate is 18.5cm from the center of the rotating table and 7.5cm above the sources. The measurements were made along two orthogonal lines across the coated wafer, one in the radial direction relative to the rotating table, the other in the tangential direction. The lines intersect at the center of the wafer. The center wavelength is taken to be midway between the half height points of the central lobe in the reflectance curve with an estimated error of  $\pm 0.03$ nm.

In Figure 4 one can clearly see a significant position dependence of the center wavelength along the radial direction. In the tangential direction there is a much smaller but still measurable shift of 0.15nm from the wafer center to the wafer edge. As all measurements were made at the same 0.8 degree angle of incidence the wavelength shifts indicate a change in the period of the multilayer across the wafer.

The observed variation of the multilayer period is consistent with the geometry of the sputtering process used to fabricate the multilayer. The dashed line in Figure 4 shows the period variation predicted by standard deposition theory for planar magnetron sputtering<sup>16</sup> with additional integration to allow for the motion of the substrates above the sputtering sources. The plasma ring diameter of the magnetron sources used in this deposition is estimated to be 41mm. The only free parameter used in this theoretical model is the position of the magnetron source which is taken to be 18.8cm from the center of the rotation table i.e., directly below the 3mm radial coordinate on the wafer. In the tangential direction we expect the finite size of the substrate rotation table to cause a small thickness change along the straight tangential line. This is indeed observed and the wavelength shift of 0.15nm is consistent with the table center to wafer center distance of 18.5cm. If a large area of uniform coating is required the thickness variations can be reduced to as little as 1-2% across several cm by the use of baffles above the sputtering source<sup>17</sup>.

Filter transmission measurements using the LPP are even simpler than multilayer reflectance measurements. As in the reflectance measurements the first scan is of the direct plasma emission over the appropriate wavelength range. The filter is then placed between the plasma and the monochromator entrance slit and a second scan is taken of the filtered plasma emission. A direct ratio of the two scans gives the filter transmission curve. Figure 5 shows the measured transmission of an aluminum filter<sup>18</sup> across the  $L_{2,3}$  edge. The filter consisted of 150nm of aluminum mounted on an 80% transmission mesh. The measured edge position agrees well with the standard value of 171.4Å and the 2Å edge width is consistent with the monochromator resolution of 1.7Å for 300μ slit widths. The measured transmission of 43% above the edge is worse than the theoretical 55% for 150nm Al<sup>19</sup> on 80% mesh. However the filter is 2 years old so we would expect some reduction in transmission due to oxidation. The measured value of 9% below the edge is higher than the theoretical 5% which we cannot yet explain.

In summary we have demonstrated a useful technique for measuring the performance of multilayer mirrors and transmission filters in the soft X-ray regime using the continuum emission from Laser-Produced Plasmas. Using this technique we have made reflectance measurements that are in excellent agreement with results obtained using synchrotron radiation. We have measured layer thickness as a function of position on a multilayer and found the behavior to be consistent with sputtering geometry used in its fabrication. We have also measured aluminum filter transmission at the Al  $L_{2,3}$  edge and found good agreement with standard results.

The measurements have a wavelength resolution limited only by the monochromator used and a reflectance/transmission resolution of 10% of the absolute value, presently limited by position stability of the copper target. Although we have presented results only for the 13nm to 18nm wavelength range, measurements should be possible over the full range of the plasma continuum emission from 1nm into the VUV.

This research was supported by the National Science Foundation.

---

### References

- 1 T. W. Barbee, Jr., AIP Conf. Proc. **75**, 131 (1981).
- 2 E. Spiller, A. Segmuller, J. Rife, and R.P. Haelbich, Appl. Phys. Lett. **37**, 1048 (1980).
- 3 G.L. Stradling, T.W. Barbee, Jr., B.L. Henke, E.M. Campbell, W.C. Mead, AIP Conf. Proc. **75**, 292 (1981).
- 4 T. W. Barbee, Jr., P. Pianetta, R. Redaelli, R. Tatchyn, T. W. Barbee, III, Appl. Phys. Lett. **50**, 1841 (1987).
- 5 J.P. Henry, E. Spiller, M. Weisskopf, Appl. Phys. Lett. **40**, 25 (1982).
- 6 J.F. Lindblom, A.B.C. Walker, T.W. Barbee, Jr., SPIE **691**, 11 (1986).
- 7 E. Spiller, in X-Ray Microscopy, ed. G. Schmahl and D. Rudolph, (Springer-Verlag, 1984), p.262.
- 8 J. A. Trail, R. L. Byer, SPIE **563**, 90 (1985).
- 9 D.J. Nagel, C. M. Brown, M.C. Peckerar, M. L. Ginter, J. A. Robinson, T. J. McIlrath, and P. K. Carroll, Appl. Opt. **23**, 1428 (1984).
- 10 R. Kodama, K. Okada, N. Ikeda, M. Mineo, K.A. Tanaka, T. Mochizuki, and C. Yamanaka, J. Appl. Phys. **59**, 3050 (1986).
- 11 P. K. Carroll, E. T. Kennedy, and G. O. Sullivan, Appl. Opt. **19**, 1454 (1980).
- 12 H. C. Gerritsen, H. van Brug, R. Bijkerk, and M. J. van der Wiel, J. Appl. Phys. **59**, 2337 (1986).
- 13 J. M. Bridges, C. L. Cromer, T. J. McIlrath, Appl. Opt. **25**, 2208 (1986).
- 14 T.W. Barbee, Jr., S.Mrowka, M.C. Hettrick, Appl. Opt. **24**, 883 (1985).
- 15 M. Kuhne, D. Stearns, N. Ceglie, Private Communication.
- 16 Handbook of Thin Film Technology, ed. L.I. Maissel and R. Glang, (McGraw-Hill, 1970), p1-56.
- 17 J. Kortright, P. Plag, R.C.C. Perera, P.L. Cowan, D.W. Lindle, B. Karlin, To be published in Nucl. Instrum. Meth.
- 18 Luxel Corporation, Friday Harbor, Washington.
- 19 D.Y. Smith, E. Shiles, M. Inokuti, Argonne National Lab. Report ANL-83-24, (1983).

## FIGURE CAPTIONS

- Figure 1** The experimental arrangement for measuring direct plasma emission (position 'a') and plasma emission reflected from the multilayer (position 'b').
- Figure 2** The direct plasma emission spectrum of the copper target from 13nm to 17nm and the plasma emission spectrum after reflection in a 62 layer pair Mo/Si multilayer with a pair thickness of 7.9nm.
- Figure 3** The experimental reflectance obtained from the scans shown in Figure 2 and a synchrotron measurement of the same multilayer.
- Figure 4** The center wavelength of the normal incidence reflectance of a 20 layer pair Mo/Si multilayer as a function of distance from the center of the substrate. Radial and tangential refer to directions relative to the rotating table used to hold the substrate during deposition. Dashed line indicates the theoretical result for the radial direction.
- Figure 5** Measured transmission of an aluminum filter across the  $L_{2,3}$  edge. The filter consists of 150nm of aluminum on an 80% transmitting mesh.

FIGURE 1

5835-2

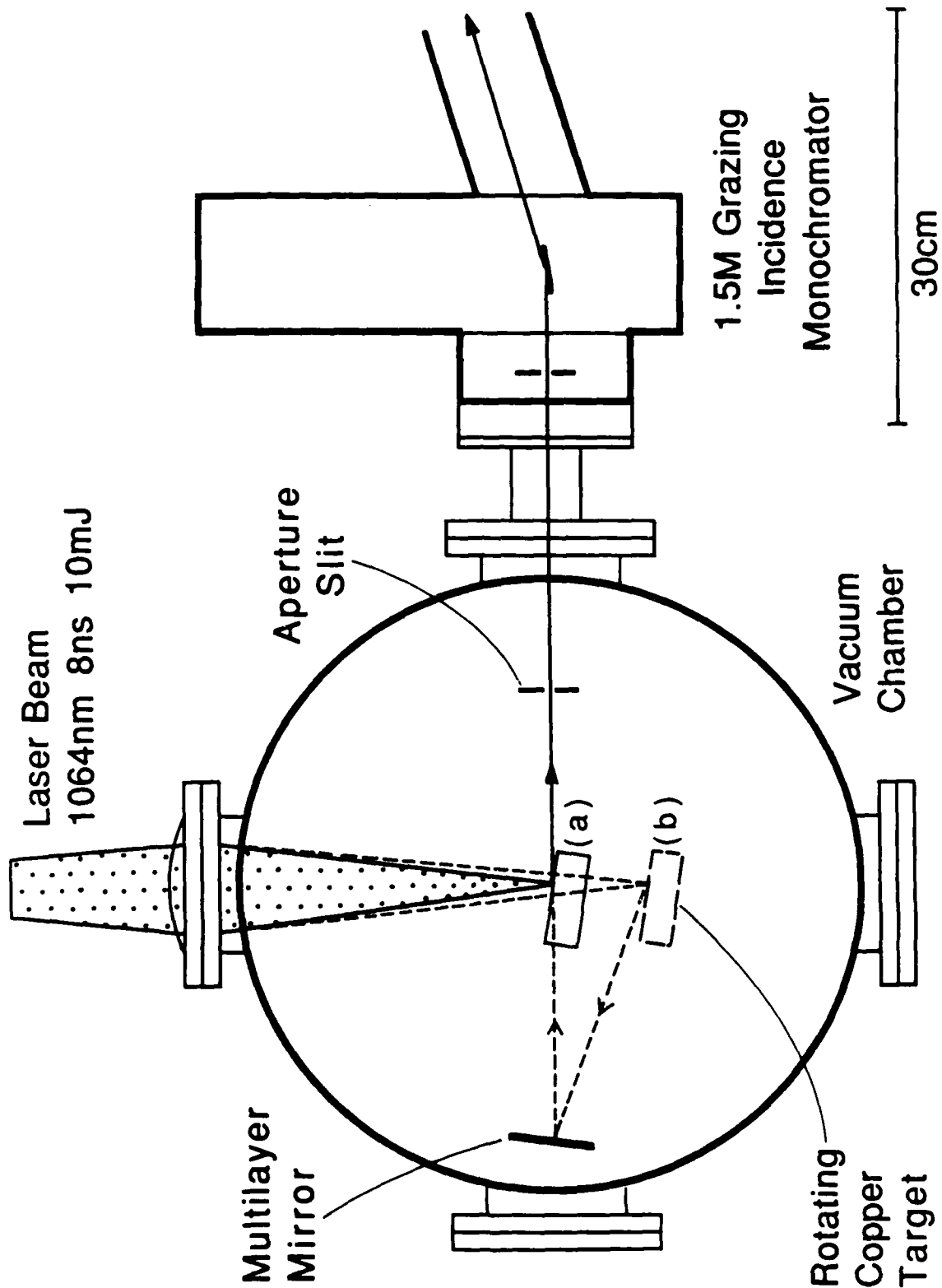


FIGURE 2

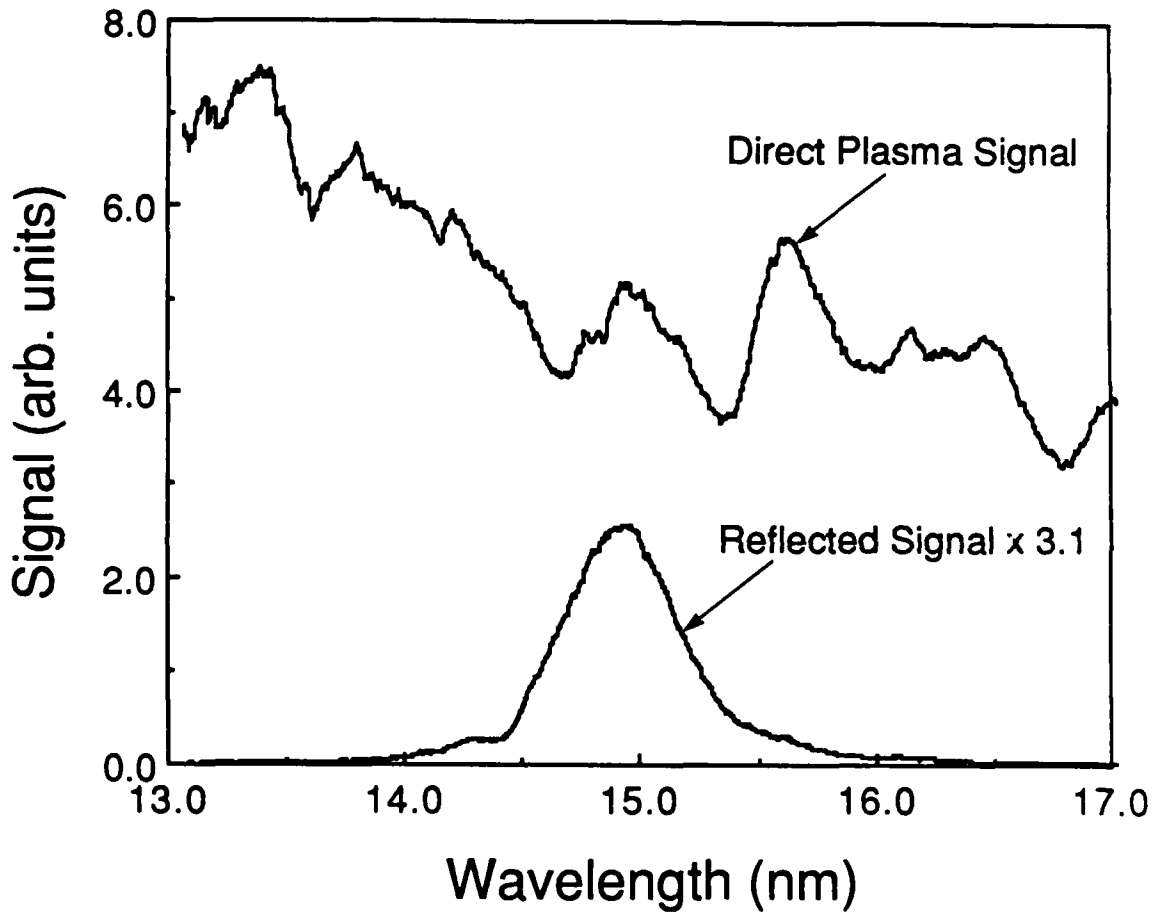
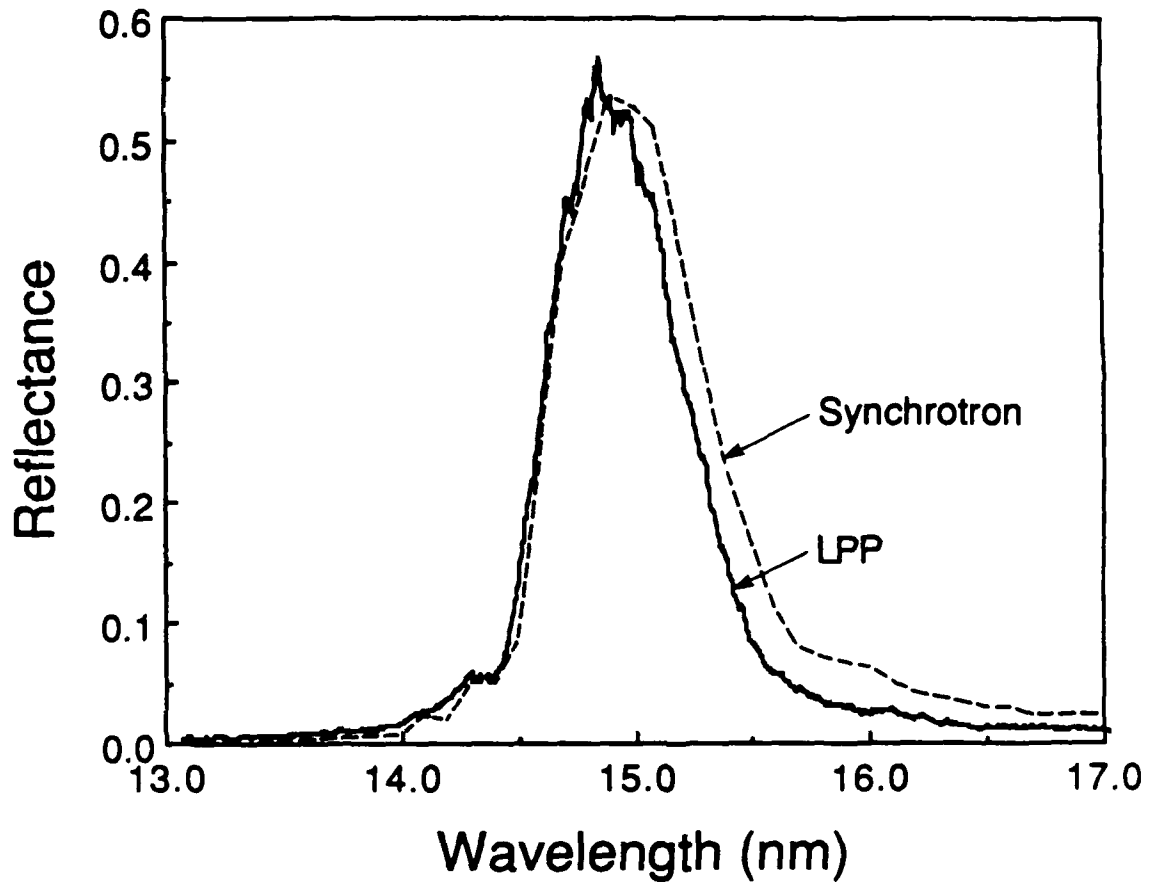


FIGURE 3



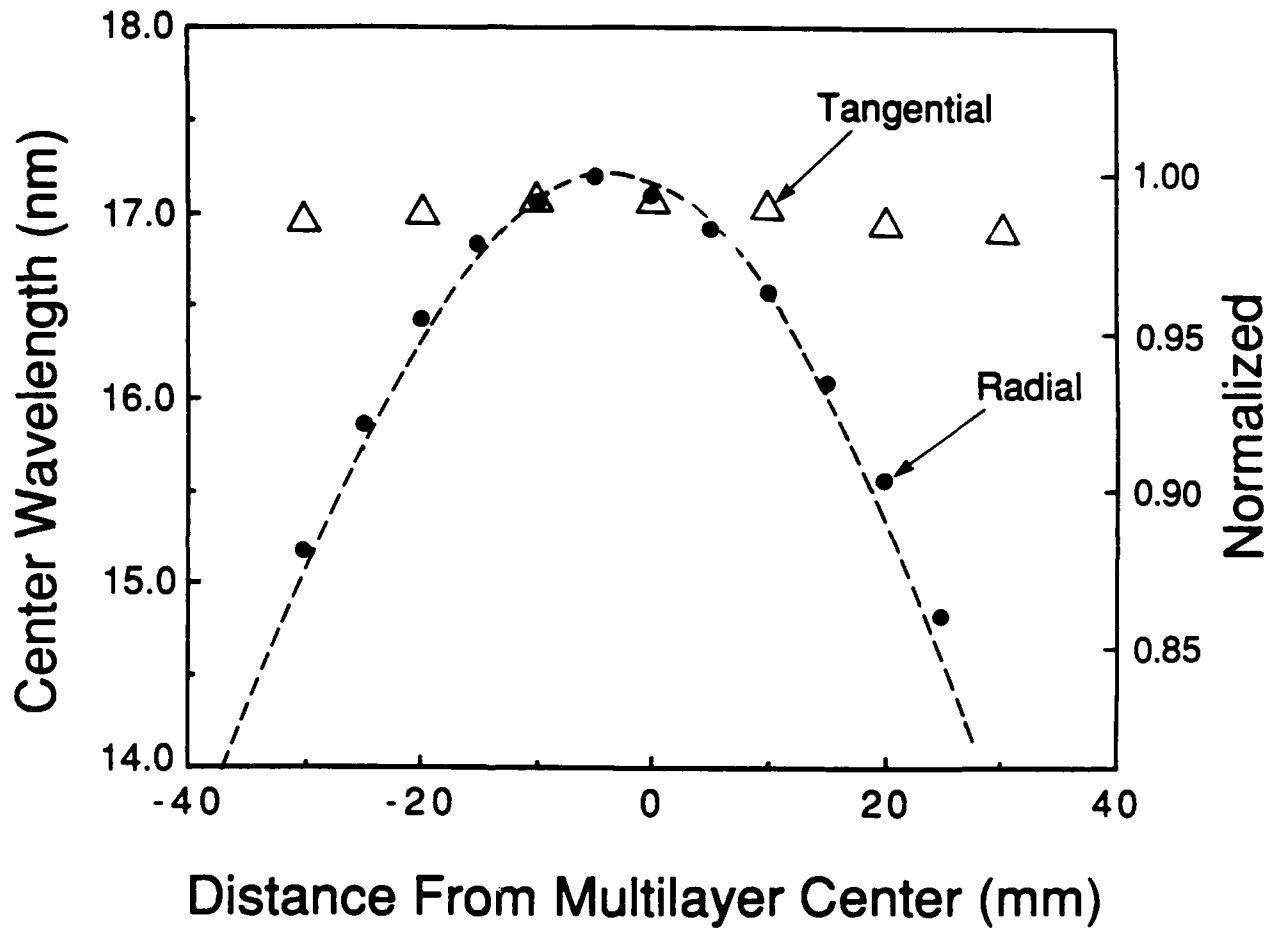
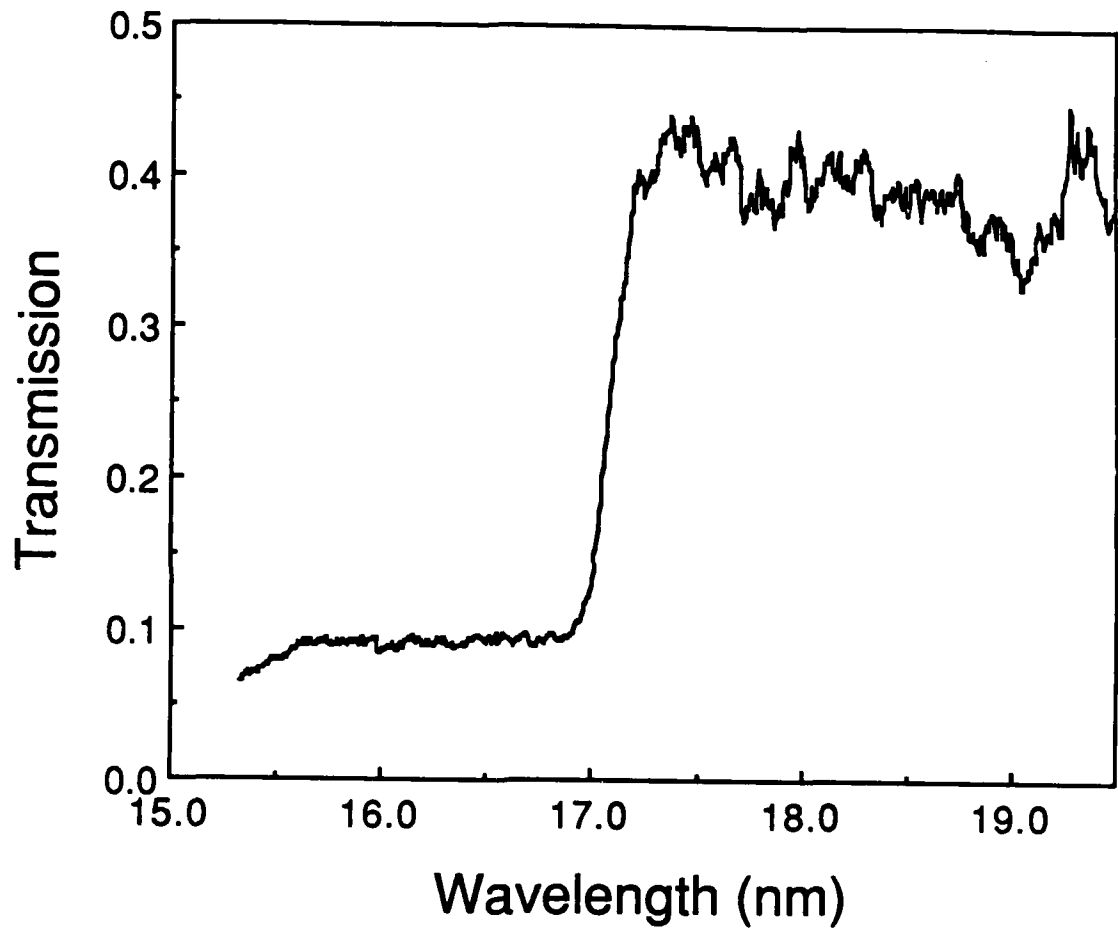


FIGURE 5



# Frequency stability and offset locking of a laser-diode-pumped Nd:YAG monolithic nonplanar ring oscillator

Thomas J. Kane,\* Alan C. Nilsson, and Robert L. Byer

Edward L. Ginzton Laboratory, Stanford University, Stanford, California 94305

Received September 9, 1986; accepted December 29, 1986

The frequency stability of laser-diode-pumped, monolithic Nd:YAG solid-state unidirectional nonplanar ring oscillators was studied by heterodyne measurements. We obtained cw single-axial- and transverse-mode power of 25 mW at 1064 nm at a slope efficiency of 19%. Two independent oscillators were offset locked at 17 MHz with frequency fluctuations of less than  $\pm 40$  kHz for periods of 8 min.

In a previous Letter we reported the operation of a monolithic, nonplanar ring resonator that was end pumped by an argon-ion laser.<sup>1</sup> The device is a monolithic block of Nd:YAG on which four reflecting facets (one spherical face with dielectric coatings; three flat, total internal reflection faces) are polished to form a nonplanar ring resonator. Because of its monolithic ring construction and built-in optical diode, the oscillator eliminates the effects of spatial hole burning, is insensitive to optical feedback, and operates in a single axial mode. The oscillator's frequency stability makes it an attractive laser source for laser radar,<sup>2</sup> coherent communications, spectroscopy and nonlinear optics,<sup>3</sup> and inertial rotation sensing.<sup>4</sup> We called the device a MISER (Monolithic, Isolated, Single-mode, End-pumped Ring), but a more descriptive acronym is SUNPRO (Solid-state, Unidirectional, Non-Planar Ring Oscillator).

The new SUNPRO is constructed from a single Nd:YAG crystal with dimensions of 12 mm  $\times$  9 mm  $\times$  3 mm. The small size and resultant reduced mode volume lead to a reduced threshold that makes pumping by a multistripe laser diode possible. The laser-diode-pumped SUNPRO is a compact, efficient source of frequency-stable 1064-nm laser radiation. In this Letter we describe experiments carried out with the laser-diode-pumped SUNPRO's: an experiment in which a laser-diode-pumped monolithic rod<sup>5</sup> was offset locked to a laser-diode-pumped SUNPRO and heterodyne measurements involving two independent, laser-diode-pumped SUNPRO's.

Figure 1(a) shows a schematic of the laser-diode-pumped SUNPRO. The SUNPRO was pumped by a 10-element, phased array of GaAlAs laser diodes, Spectra Diodes Laboratories (SDL) Model 2420-C,<sup>6</sup> that emitted 200 mW of 810-nm radiation in a two-lobed far-field pattern. The temperature of the laser diode was controlled with a thermoelectric cooler to tune the emission wavelength to the strong Nd:YAG absorption band at 809 nm. The output of the SDL 2420-C was collimated and focused onto the spherical face of the Nd:YAG block as shown in Fig. 1(a).

The SUNPRO operates in a TEM<sub>00</sub> spatial mode with dimensions fixed by the 50-mm radius of curva-

ture of the dielectric-coated surface and the 28.54-mm path length of the ring. Output is taken through the curved surface, which is coated for normal-incidence reflectivity of 99.1% at 1064 nm. The measured threshold was 16.9 mW, and the slope efficiency was 19.6%. The SUNPRO, which incorporates an optical diode<sup>7,8</sup> into its resonator by virtue of its nonplanar light path and the applied magnetic field, oscillates unidirectionally in a single axial mode.

Figure 1(b) shows a schematic of the experimental setup used for the offset-locking experiments. A laser-diode-pumped monolithic rod laser was offset locked to a laser-diode-pumped SUNPRO. The output beams of the two laser-diode-pumped Nd:YAG lasers were focused into two single-mode optical fi-

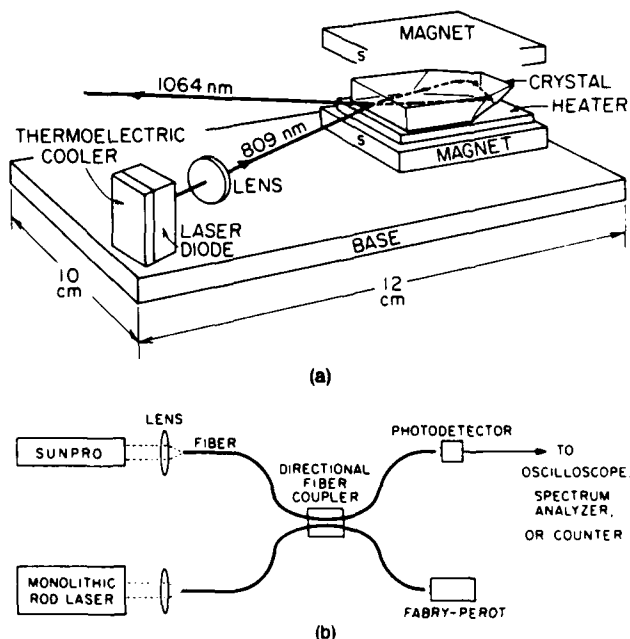


Fig. 1. (a) Schematic of laser-diode-pumped SUNPRO. (b) Experimental setup for heterodyne measurements and offset locking.

bers, combined by a directional fiber coupler,<sup>9</sup> and mixed on an InGaAs photodetector. The beat signal from the photodetector was then sent to a frequency counter, oscilloscope, or spectrum analyzer.

The frequency difference between the two lasers was varied by changing the temperature of the monolithic rod while holding the temperature of the SUNPRO constant. A monolithic resonator of Nd:YAG changes its resonant frequency by  $-3.1 \text{ GHz}/^\circ\text{C}$  at room temperature. We used circuitry to count the frequency of the beat signal, compare it with a desired frequency difference, and generate an error signal that was then fed back to the temperature controller of the monolithic rod laser.<sup>10</sup> By this technique we were able to offset lock the SUNPRO and the monolithic rod laser.

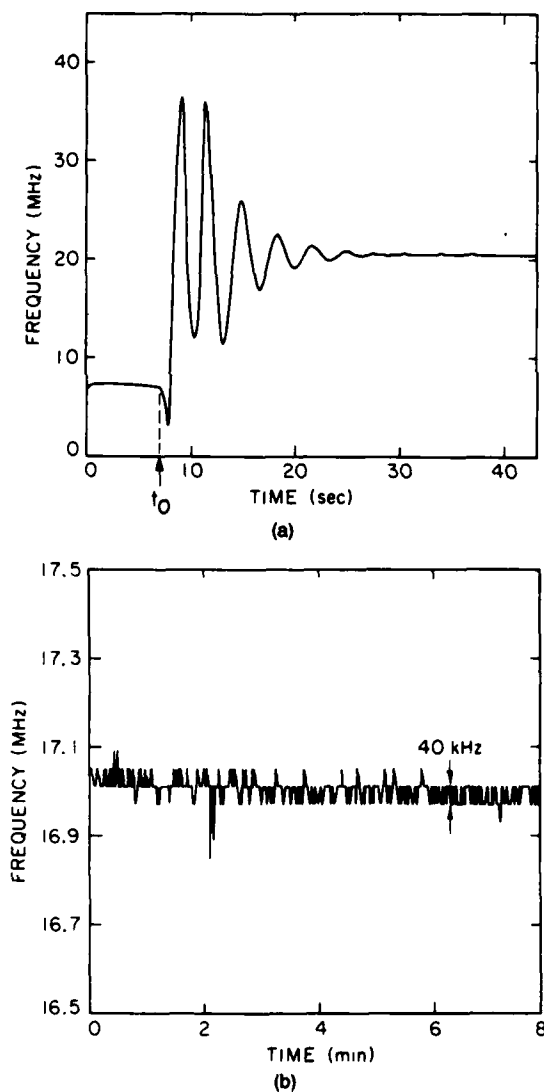


Fig. 2. (a) Offset-frequency-locking transient of laser-diode-pumped monolithic rod and SUNPRO. Locking circuit turned on at  $t_0$ . (b) Stable heterodyne signal between offset-locked oscillators as measured by frequency-counting circuit. Frequency resolution of the counting circuit is  $\pm 40 \text{ kHz}$ .

Figure 2(a) shows the capture transient and the subsequent locked performance of the SUNPRO and miniature monolithic rod laser at an offset frequency of 21 MHz. Figure 2(b) shows the frequency difference between the two lasers offset locked at 17 MHz and controlled to within  $\pm 40 \text{ kHz}$  for 8 min. The data shown in Figure 2(b) were obtained by counting the zero crossings of the beat signal during a fixed time interval of  $25 \mu\text{sec}$ , yielding a mean frequency data point that was relayed to computer storage. The counting circuit was reset and the process repeated. The total number of data points and the time interval between data points were variable. The fixed counting interval of  $25 \mu\text{sec}$  and the counting accuracy of  $\pm 1$  count limited the frequency resolution of any data point to  $\pm 40 \text{ kHz}$ .

The SUNPRO showed better resistance than the monolithic rod laser to instabilities caused by reflections from the faces of the optical fibers. To attain a stable heterodyne signal, the output of the monolithic rod laser was attenuated by 30 dB before it was focused into the fiber, whereas the SUNPRO required no attenuation. The SUNPRO has four nondegenerate eigenmodes (two eigenpolarizations for each of two directions of propagation around the ring), and unidirectional oscillation occurs for the eigenmode with the largest eigenvalue modulus.<sup>11</sup> Output radiation retroreflected back into the SUNPRO travels opposite the oscillating mode and is offset in frequency from the eigenfrequencies of the possible retropropagating modes. These two effects reduce the influence of optical feedback on the SUNPRO relative to the influence on a standing-wave oscillator.

The offset-locking experiment demonstrated the extreme frequency stability of laser-diode-pumped monolithic laser sources but did not differentiate between the frequency fluctuation contributions of the two different oscillators. To address this question, we constructed a second SUNPRO and performed a heterodyne experiment using the two SUNPRO's. The setup shown in Figure 1(b) was used with the monolithic rod laser replaced by the second SUNPRO. Because of the larger thermal time constant of the SUNPRO, we did not offset lock the devices but instead explored the beat frequency between two free-running oscillators.

A rf spectrum-analyzer trace of the heterodyne signal from the two SUNPRO's is shown in Fig. 3(a). This scan shows a central peak near 9 MHz and relaxation oscillation sidebands at  $\pm 70 \text{ kHz}$  from the central peak. The relaxation oscillation sidebands are 35 dB down from the amplitude of the central beat frequency. The key feature of the scan is the spectrum-analyzer-limited 3-kHz full width at the  $-3\text{-dB}$  points of the beat note. We conclude that each of the free-running SUNPRO's has a linewidth of less than 3 kHz over the 100-msec spectrum analyzer sweep time. Frequency jitter and drift in the beat signal precluded meaningful measurements for the sweep times required to give resolution better than 3 kHz.

Using the frequency-counting circuit to analyze the long-term behavior of the heterodyne signal gave the data shown in Fig. 3(b). Since the SUNPRO's were

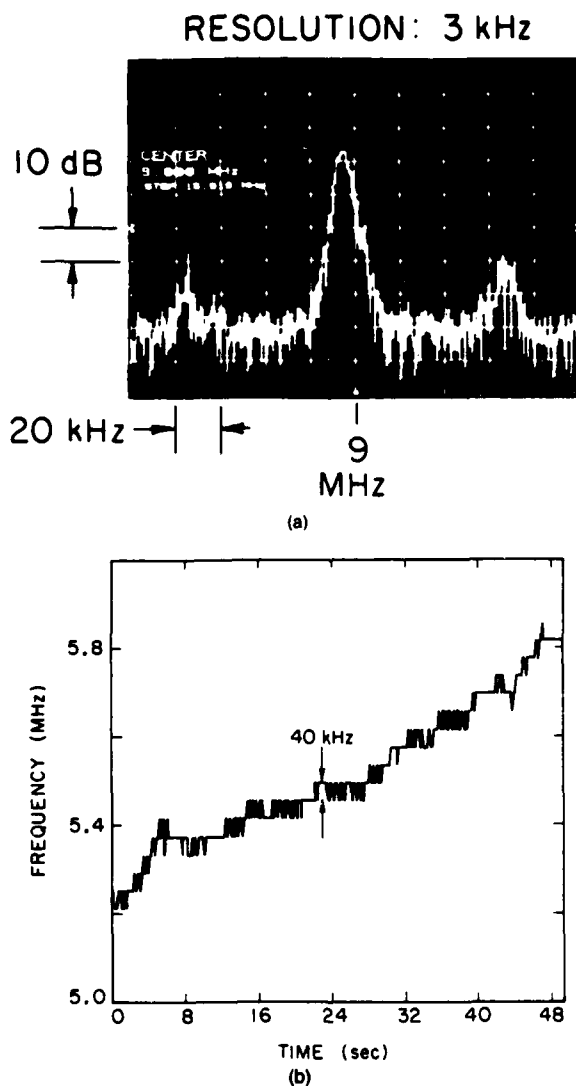


Fig. 3. (a) Spectrum-analyzer trace of heterodyne signal between two free-running SUNPRO's, showing a central peak at the 9-MHz offset frequency and relaxation oscillation sidebands. Full width at the  $-3$ -dB points of the central peak is 3 kHz, limited by the resolution bandwidth of the spectrum analyzer. (b) Heterodyne signal between free-running SUNPRO's, measured by the frequency-counting circuit. Note the uncompensated drift rate of 12 kHz/sec.

not locked, there was a large uncompensated thermal drift of 12 kHz/sec. Apart from the drift, however, the individual data points show behavior similar to that observed with the offset-locked oscillators. Careful thermal design will permit offset locking of SUNPRO's in the future.

The multistripe laser-diode arrays used as pumps in these experiments are not optimal for producing frequency-stable operation in SUNPRO's. Fluctuations in the output power and the spatial mode of the phased array cause frequency fluctuations in the output of a SUNPRO. For example, an increase of 100  $\mu$ W of heat input for 100  $\mu$ sec produces a temperature

increase of 4  $\mu$ K in the  $10^{-3}$ -cm<sup>3</sup> mode volume of the SUNPRO. Multiplying by Nd:YAG's thermal tuning coefficient of  $-3.1$  GHz/K gives a frequency shift of 12.4 kHz. This simple calculation shows the extreme sensitivity of Nd:YAG to thermally induced frequency shifts and thus underscores the importance of stable pumping. In future experiments we plan to reduce the Nd:YAG SUNPRO dimensions, thereby reducing the threshold pumping power to permit operation with single-stripe, single-mode laser diodes.

In summary, we have demonstrated that the diode-pumped SUNPRO offers high single-mode output power in a compact device with excellent frequency stability. We have amplified the output of a SUNPRO by 60 dB, making available high-power, narrow-linewidth radiation.<sup>12</sup> This narrow-linewidth, high-power source has already performed successfully in a coherent laser radar experiment<sup>13</sup> and will prove similarly useful as a pump source for nonlinear-optics experiments. That the SUNPRO can be laser-diode pumped also makes it attractive for spaceborne experiments in which compactness, low power consumption, and reliability are essential. We are currently investigating the fundamental linewidth limitations of the SUNPRO.

This research was supported by the National Aeronautics and Space Administration.

\* Present address, Lightwave Electronics Corporation, 897-4A Independence Avenue, Mountain View, California 94043.

## References

1. T. J. Kane and R. L. Byer, *Opt. Lett.* **10**, 65 (1985).
2. T. J. Kane, B. Zhou, and R. L. Byer, *Appl. Opt.* **23**, 2477 (1984).
3. R. L. Byer, G. J. Dixon, T. J. Kane, W. J. Kozlovsky, and B. Zhou, in *Laser Spectroscopy VII*, T. W. Hänsch and Y. R. Shen, eds. (Springer-Verlag, Berlin, 1985), p. 350.
4. D. Z. Anderson, *Sci. Am.* **254**, 94 (1986).
5. B. Zhou, T. J. Kane, G. J. Dixon, and R. L. Byer, *Opt. Lett.* **10**, 62 (1985).
6. Spectra Diodes Literature, Spectra Diodes Laboratories, 3333 North First Street, San Jose, Calif. 95134.
7. T. F. Johnston and W. Proffitt, *IEEE J. Quantum Electron.* **QE-16**, 483 (1980).
8. T. J. Kane and R. L. Byer, "Solid-state non-planar internally reflecting ring laser," U.S. Patent No. 4,578,793, March 25, 1986.
9. R. A. Bergh, G. Kotler, and H. J. Shaw, *Electron. Lett.* **16**, 280 (1980).
10. T. J. Kane, Ph.D. dissertation (Stanford University, Stanford, California, 1986).
11. H. Statz, T. A. Dorschner, M. Holtz, and I. W. Smith, in *Laser Handbook*, M. L. Stitch and M. Bass, eds. (Elsevier, New York, 1985), Vol. 4, p. 229.
12. T. J. Kane, W. J. Kozlovsky, and R. L. Byer, *Opt. Lett.* **11**, 216 (1986).
13. T. J. Kane, W. J. Kozlovsky, R. L. Byer, and C. E. Byvik, "Coherent laser radar at 1.06  $\mu$ m using Nd:YAG lasers," submitted to *Opt. Lett.*